

Large Scale Structure at 24μm from Counts-in-Cells in the SWIRE Survey

Frank Masci^{1,2}, David Shupe^{1,2}, Fan Fang^{1,2}, Tracey Evans², Russ Laher^{1,2}, Michael Rowan-Robinson³, Tom Babbedge³, Mattia Vaccar³, Maria Polletta⁵, Carol Lonsdale², Kevin Xu², Sebastian Oliver⁴, Jason Surace^{1,2}, Deborah Padgett^{1,2} and Harding E. Smith⁵



¹Spitzer Science Center (SSC), California Institute of Technology
²Infrared Processing and Analysis Center (IPAC), California Institute of Technology
³Blackett Laboratory, Imperial College London
⁴Astronomy Center, CPES, University of Sussex
⁵Center for Astrophysics and Space Sciences, UCSD
fmasci@ipac.caltech.edu



Summary and Goals

- The *Spitzer* Wide-area InfraRed Extragalactic legacy program (SWIRE; Lonsdale et al. 2003, 2004) is expected to detect over two million galaxies at infrared wavelengths from 3.6 to 160μm over 49 deg². The survey is intended to study galaxy evolution, the history of star formation and accretion processes, and due to its large sampled volume, how these are influenced by galaxy clustering and environment on all scales.
- We present initial results of galaxy clustering at 24μm by analyzing statistics of the projected galaxy distribution from *counts-in-cells*. This study focuses on the **ELAIS-North1 SWIRE field**. The sample covers ~5.9 deg² and contains 24,715 sources detected at 24μm to a limit of 250μJy (~5.4s in the lowest coverage regions). This flux limit corresponds to a 90% completeness. Reliability of each 24μm detection was ensured by requiring an IRAC 3.6μm association with SNR > 10s (where 0.6 = s/μJy = 1.0) and separation < 2 arcsec.
- Why counts-in-cells?** The (normalized) galaxy count distribution gives the probability of finding *N* galaxies in a randomly placed cell of given size. All higher order moments and *n*-point correlations can then be derived therefrom. The two-point correlation function is simply related to the variance, the three-point to the skewness and so on. The method does not require binning (like the traditional method), no random comparison sample is needed, has better SNR properties (due to large scale averaging) and systematic effects from catalog boundaries are minimized.

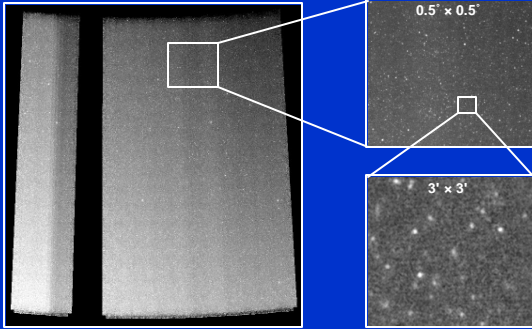


Figure 1: SWIRE ELAIS-N1 24μm mosaic. The gap is due to Spitzer going in safemode on January 25, 2004 resulting in the loss of 5 AORs. These were re-observed in July.

- This study is the first of its kind at this wavelength and sensitivity, reaching a factor of ~1000 deeper in flux density than the IRAS 25μm galaxy surveys. We have explored clustering statistics as a function of 3.6 – 24μm color and 24μm flux density by:
 - Comparing distributions of galaxy counts-in-cells with the quasi-equilibrium gravitational clustering model of Saslaw & Hamilton (1984) to constrain the dimensionless parameter $b = -W/2K$ (effectively the ratio of gravitational correlation energy to kinetic energy of peculiar velocities) as a function of angular scale.
 - Computing the second and third moments of the galaxy distribution (variance and skewness) and used these to test the hierarchical model for the formation and non-linear growth of cosmic structure.
 - Computing the two-point autocorrelation function using a power-law inversion of the angular-averaged variance from counts-in-cells.
 - Deprojecting the angular autocorrelation function using a photometric redshift distribution and Limber's (1959) equation to obtain estimates of three-dimensional clustering for all flux and color subsamples.
- Selection functions, reliability, star-galaxy separation analysis (see e.g., Figure 2) and the results presented herein will appear in a forthcoming paper (Masci et al., 2004, ApJ in preparation).

Galaxy Clustering Results

- Counts are performed in circular cells of angular diameter 0.05 to 0.7°, corresponding to comoving spatial scales of 1 - 15h⁻¹ Mpc at the median (photometric) redshift of $z=0.46$. Statistics are analyzed in four broad flux and color subsamples. Figure 3 shows distributions of galaxy counts within a fixed cell diameter of 0.4° for all subsamples. Solid lines are fits of quasi-equilibrium gravitational clustering model of Saslaw & Hamilton (1984). This model is parameterized by the single parameter $b = -W/2K$. Dashed curves are Poisson predictions. On this scale, the distributions are clearly consistent with non-Poisson (correlated) sampling.

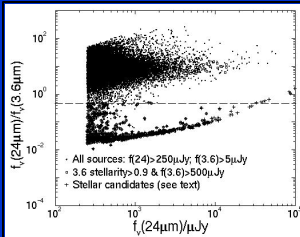


Figure 2: Ratio of 24-3.6μm flux density versus 24μm flux density. Sources marked with a "+" are flagged as stellar.

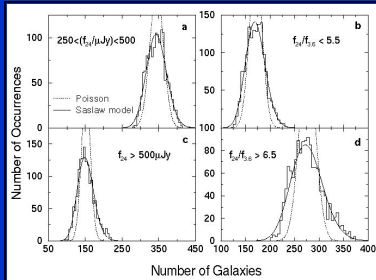


Figure 3: Galaxy count distributions for cell diameter of 0.4°.

- Values of the *b* parameter, the ratio of gravitational correlation energy to kinetic energy of peculiar velocities (from fits of the Saslaw & Hamilton(84 model), approach values of 0.4-0.6 on the largest scales probed, consistent with studies in the optical. The blue and red subsamples have *b* values of 0.40±0.02 and 0.60±0.03 respectively, suggesting that redder galaxies are more strongly clustered (see Figure 4).
- We have also measured the angular RMS fluctuation ($\langle \delta N \rangle$) and skewness from the galaxy distributions and detected significant deviations from the predictions of Poisson sampling at angular scales > 0.1° (see Figure 5).

- From moments of counts-in-cells distributions, we have estimated *area-averaged* two and three-point correlation functions: $\langle w_2(\theta) \rangle$ and $\langle w_3(\theta) \rangle$ respectively. The full sample two-point correlation function is shown in Figure 6 and for all subsamples in Figure 7. In Figure 6, we compare with the 2-point correlation fit derived using the traditional binning method. Solid lines are linear regression fits of the form $\langle w_2(\theta) \rangle = C(\theta)\theta^{1-a}$ where *C*(θ) is a non-analytic function of θ.
- From Figure 7, galaxies with redder near-to-mid-IR colors appear more clustered as seen in their correlation amplitude on angular scales > 0.2°. This is also seen if the color subsamples are binned as a function of redshift (see Figure 8).

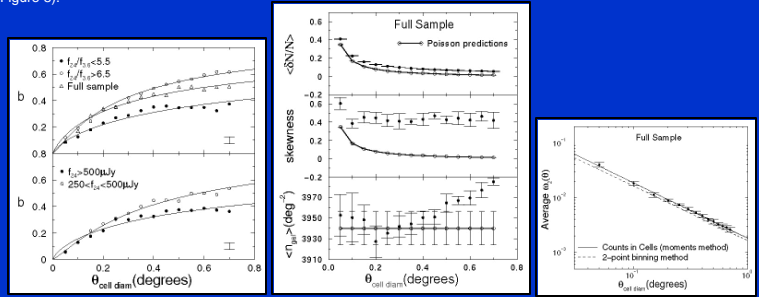


Figure 4: ($b = -W/2K$)

Figure 5

Figure 6

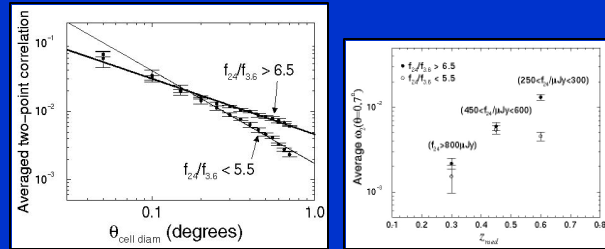


Figure 7

Figure 8

Figure 8: Two-point correlation function estimates averaged on 0.7° scales for three median photometric redshift bins corresponding to the flux density ranges shown in parenthesis

- The skewness is found to be related to the variance through $\langle w_3(\theta) \rangle = S_3 \langle w_2(\theta) \rangle^2$, with $a = 1.75 \pm 0.13$ for the full sample. This is marginally consistent with the hierarchical model for the non-linear growth of Gaussian primordial fluctuations under gravity which predicts $a = 2$ exactly. We also find that the hierarchical amplitude $S_3 = 9 \pm 2$ is scale invariant and consistent with this model.

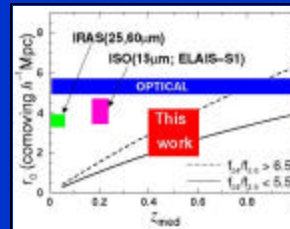


Figure 9: Comoving correlation length r_0 as a function of the median redshift of a population.

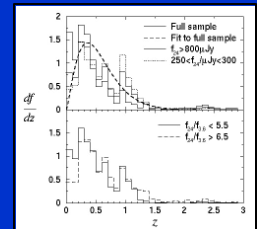


Figure 10: Photo-*z* distributions normalized to unity within each subsample.

- Using photometric redshift distributions (from the photo-*z* code of Rowan-Robinson et al. 2003) and assuming stable clustering, we have inverted Limber's equation and found spatial comoving correlation lengths of $r_0 \sim 2.15$ to 3.75 h⁻¹ Mpc across all subsamples (see Figure 9). The blue and red subsamples have the lowest and highest r_0 values respectively. These estimates are smaller than those derived from optical surveys, but in agreement with results from IRAS and ISO in the mid-infrared. This extends the notion to higher redshifts that infrared selected surveys show weaker clustering than optical surveys. Uncertainties in r_0 are dominated by uncertainties in the redshift distribution.
- Comparing clustering statistics for blue and red subsamples (Figures 7, 8 and 9), galaxies with redder near-to-mid-IR colors appear more clustered by factors of ~3 in their correlation amplitude. This suggests that merger driven starbursts may be playing an important role in the mid-infrared excess population at $z > 0.5$.

Table 5: Clustering analysis results

Subsample	$\langle b \rangle$	$\langle S_3 \rangle$	$\langle a \rangle$	$\langle r_0 \rangle$	$\langle r_0 \rangle$ (h ⁻¹ Mpc)	$\langle r_0 \rangle$ (h ⁻¹ Mpc)
Full Sample	0.50 ± 0.02	9 ± 2	1.75 ± 0.13	2.15 ± 0.15	2.15 ± 0.15	2.15 ± 0.15
Blue (f ₂₄ /f _{3.6} < 5.5)	0.40 ± 0.02	9 ± 2	1.75 ± 0.13	2.15 ± 0.15	2.15 ± 0.15	2.15 ± 0.15
Red (f ₂₄ /f _{3.6} > 6.5)	0.60 ± 0.03	9 ± 2	1.75 ± 0.13	2.15 ± 0.15	2.15 ± 0.15	2.15 ± 0.15